Optimal adjustment of the FAST active reflecting surface based on a working paraboloid adjustment model

Zhangyi Kong[1,*], Tianyuan Huo[1], Chenyu Nan[2]

[1]College of Science, Zhejiang University of Technology, Zhejiang, China, 310023

[2]College of Mechanical Engineering, Zhejiang University of Technology, Zhejiang, China, 310023

*Corresponding author: 201906110710@zjut.edu.cn

Abstract. FAST is the world's largest single-aperture radio telescope developed independently by China, which adopts innovatively the active reflecting surface technology to realize real-time adjustment of the reflecting surface and dynamic tracking of celestial objects. In this paper, the ideal paraboloid for observing celestial objects is investigated in conjunction with the adjustment factors of the reflecting panel, and the adjustment of the working paraboloid is optimally designed. To address problem one, this paper first cognizes the ideal paraboloid, establishes four criteria that the ideal paraboloid should satisfy, and simplifies the problem in two dimensions based on symmetry. For problem two, this paper firstly establishes a mathematical model for solving the equations of the ideal paraboloid in the general case based on the results of problem one, using the coordinate transformation method.

Keywords: Reflective Surface Optimization, Celestial Objects, Mesh Traversal Method, Coordinate Transformation, Feature Points.

1. Introduction

FAST is the world's largest single-aperture radio telescope with the highest sensitivity, developed independently by China, which innovatively adopts adjustable active reflector technology, allowing real-time adjustment of the active reflector shape according to the position of the observed object, thus achieving automatic tracking of the observed object[1-2]. The strategy for adjusting the shape of the active reflecting surface depends on the position of the observed object and the reception requirements for converging the reflected signals in the feeder module, but also on the constraints of the support structure on the shape adjustment[3]. Therefore, it is important to establish a mathematical model to determine an ideal reflecting paraboloid, and then develop a reasonable strategy to adjust the shape of the reflecting surface so that the working paraboloid is close to the ideal paraboloid, in order to improve the information reception of the feeder module and thus the sensitivity and resolution of FAST[4-6].

2. The establishment and solution of model

2.1 Establishment of an ideal parabolic optimization model

(1) Two-dimensional simplification of the ideal paraboloid

Based on the symmetry of the reference sphere and the rotating paraboloid, one can consider solving for the ideal paraboloid in the profile, which can be obtained by rotating the ideal paraboloid around the axis of symmetry for one week. Under the condition that the position of the celestial body to be observed in this question is α=0°, β=90°, the equation of the ideal paraboloid can be set as:

$$x^2 = 2pz + q \tag{1}$$

where p,q are parameters to be determined and can be optimally solved by the subsequent optimization model. The focal length, vertex coordinates and endpoint coordinates of the parabola (by symmetry, only the left endpoint is considered below) are as follows

$$\text{Focal length:} f = \frac{p}{2} \tag{2}$$

$$\text{Vertex coordinates:} v = \left(0, -\frac{q}{2p}\right) \tag{3}$$

$$\text{Endpoint coordinates:} \ E\left(-150, \frac{22500-q}{2p}\right) \tag{4}$$

Furthermore, in the profile, the equation of the line of intersection between the reference sphere and the profile can be expressed as

$$x^2 + z^2 = R^2 \tag{5}$$

where R is the radius of the sphere, $R = 300m$

(2) Quantitative analysis of the ideal state

The "ideal state" of an ideal parabola is quantified in this paper according to the four criteria proposed above for the perception of an ideal paraboloid as follows.

1. Analysis of the reflected signal reception

For any point on an ideal parabola other than the vertex, consider the case where the reflected signal is received. Under the assumption that both the electromagnetic signal and the reflected signal are considered to propagate in a straight line, the reflection of the signal obeys the law of reflection of light[7].

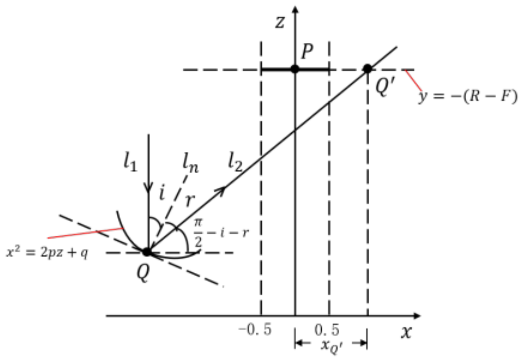

Figure 1. The reflection of reflected signal

According to the geometric properties of the parabola, the slope of the normal l_n is $k_n = -\frac{p}{x}$. Combining the geometric relationships in the diagram, we obtain the angle of incidence satisfies the trigonometric relationship:

$$tan\, i = -\frac{x}{p} \tag{6}$$

According to the law of reflection of light, the angle of reflection is equal to the angle of incidence, then we have

$$r = i = arc\,tan\left(-\frac{x}{p}\right) \tag{7}$$

The angle between the reflected ray l_2 and the positive semi-axis of the x-axis is $\frac{\pi}{2} - i - r$. Therefore, the slope of the reflected ray is

$$k_2 = \tan\left(\frac{\pi}{2} - i - r\right) = -\frac{p^2 - x^2}{2px} \tag{8}$$

On the profile, the projection of the effective region is a line segment with a linear equation of

$$z = F - R \tag{9}$$

Let the intersection of the reflected ray and the projection line of the effective area be the reflection point Q'. The longitudinal coordinates of the reflection point can be obtained by combining the equations of the reflected ray and the projection line of the effective area:

$$\begin{cases} z_{Q'} - z_Q = k_2\left(x_{Q'} - x_Q\right) \\ z_{Q'} = F - R \end{cases} \tag{10}$$

After getting the reflection point, the coordinates of $\left(x_{Q'}, z_{Q'}\right)$, the reflected signal is known to be received as follows

$|x_{Q'}| \le 0.5 \rightarrow$ Reflected signal enters valid area and is received

$|x_{Q'}| > 0.5 \rightarrow$ Reflected signal does not enter the valid area and is not received

2. Analysis of the range of the parabolic fall

The expansion and contraction of the actuator limits the values of the vertical coordinates of the points on the parabola, so to simplify the model, only the parabola is considered here. The case where the vertex of the object *V* is limited by the retraction of the actuator, this limitation can be expressed by the inequality:

$$-300 - 0.6 \leq -\frac{q}{2p} \leq -300 + 0.6 \tag{11}$$

According to the above equation, after a certain parameter p has been determined, the range of values of the parameter q can be narrowed down and the optimal solution can be found further by traversal.

3. Analysis of the maximum expansion of the actuators

The expansion of the actuator is in the radial direction, in the given right-angle coordinate system, for any point on the parabola, under the assumption that the point is the premise of the main rope node, its corresponding actuator expansion is

$$d = \left|\sqrt{x^2 + z^2} - R\right| \tag{12}$$

From this, the maximum expansion of the actuator is obtained:

$$d_{max} = \max_{(x,z)\in\Omega}\left|\sqrt{x^2 + z^2} - R\right| \tag{13}$$

where d_{max} denotes the maximum stretch of the actuator and Ω is the set of parabolic points. After determining a set of parabolic parameters, the parabolic equation and parabolic point set can be obtained, which in turn gives the maximum retractable volume of the actuator for that parameter condition. Thus, d_{max} is actually a function of p, q.

According to equation, the parabolic parameter p is related to the focal length of the parabola f: $p = 2f$. According to the question, in the ideal parabola, the focal length should be the difference between the radii of the two spheres *F*, but considering that the effective area is a disc area, it is possible to allow the actual focal length to be different from the ideal value. There is a small deviation without affecting the reception of the full reflected signal. Therefore, this paper considers the case where the focal length can be taken within a small interval, i.e.:$F - \Delta f \leq f \leq F + \Delta f$

The range of values for the parameter p is then:

$$2(F - \Delta f) \leq p \leq 2(F + \Delta f) \tag{14}$$

Once the range of values for p is obtained, for each p the corresponding parameter can be further obtained based on the analysis of the parabolic fall point above the range of values of q.

(3) Ideal parabolic optimization model

Integrating the above analysis of the ideal parabola, this paper establishes an optimization model with the constraint that all reflected signals are received and the objective function of minimizing the maximum stretch of the actuator.

(a) Decision-making variables

The practical requirement of this problem is to optimally adjust the shape of the working paraboloid of the active reflective surface, so the decision variables are the parameters of the parabolic equation p, q.

(b) Binding conditions

Considering that the optimization objective is set to minimize the maximum expansion, the expansion constraint of the actuator is not considered in the constraints in this paper to simplify the computational solution of the model. As a result, the only constraint is determined to be the satisfaction that all reflected signals can be reflected into the effective region. According to symmetry and continuity, it is only necessary to satisfy that the reflection point corresponding to the left end point *E* falls within the projection line segment of the effective region, i.e.

$$|x_{E'}| \leq 0.5 \tag{15}$$

Where $x_{E'}$ is the point of reflection corresponding to the left endpoint of the parabola *E* , the horizontal coordinate of E' is calculated as described in the analysis of reflected signal reception above.

(c) Target function

Under the premise of satisfying the above constraints, it is desired to minimize the maximum actuator expansion and contraction so as to reduce the burden on the support structure while satisfying the actuator expansion and contraction constraints and at the same time obtaining a better dynamic tracking effect. Therefore, the following objective function is obtained in this paper:

$$mind_{max}(p,q) = \max_{\substack{p,q \\ (x,z)\in\Omega}} \left|\sqrt{x^2+z^2}-R\right| \tag{16}$$

In summary, an optimal model of the ideal parabola is developed as follows.

$$\text{s.t.}\begin{cases} |x_{E'}| \le 0.5 \\ 2(F-\Delta f) \le p \le 2(F+\Delta f) \\ 299.4 \times 2p \le q \le 300.6 \times 2p \end{cases} \tag{17}$$

By choosing a suitable focal deviation *Δf* and performing a grid traversal of the decision traversal *p, q,* the optimal ideal paraboloid parameters and the corresponding minimum actuator maximum expansion can be solved for.

(d) Parametric solutions for ideal parabolas

In this paper, a grid traversal method is used to traverse the parabolic optimization model to solve it.

First, the ideal focal length $F = 0.466 \times 300 = 139.8(m)$ can be calculated from the focal diameter ratio and the spherical radius. Combining this ideal focal length with the value of $\Delta f = 2.5m$ as the focal length deviation, the range of the parameter p is

$$274.6 \le p \le 284.6 \tag{18}$$

In taking the median $p = 279.6$, the range of values of q

$$167424.48 \le q \le 168095.52 \tag{19}$$

In order to reduce the computational effort while maintaining accuracy, the grid traversal step is designed to be $\Delta p = 0.001$, $\Delta q = 1$. The final optimal solution and the optimal objective function values are shown in the table (all units are SI).

Table 1. Table of results for the ideal parabola of Problem

parameter	p	q	d_{max}
Value	280.274	1.683520712×10^5	0.3360

The parabolic equation of the ideal parabola is further obtained as follows.

$$x^2 = 560.548z + 168352.0712 \tag{20}$$

From this, the parabolic equation of the ideal paraboloid is

$$x^2 + y^2 = 560.548z + 168352.0712 \tag{21}$$

At this point, the coordinates and focal lengths of the vertices of the ideal paraboloid are shown in the table below (in *m*).

Table 2. Table of parameters related to the ideal paraboloid of the model

parameter	x_v	y_v	z_v	f
Value	0	0	−300.3348	140.137

The ideal parabolic profile (ideal parabola) and the three-dimensional top view obtained are shown in Fig. 2 and Fig. 3.

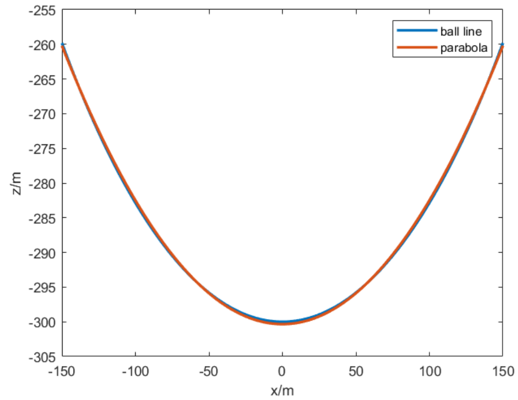

Figure 2. Ideal paraboloid section

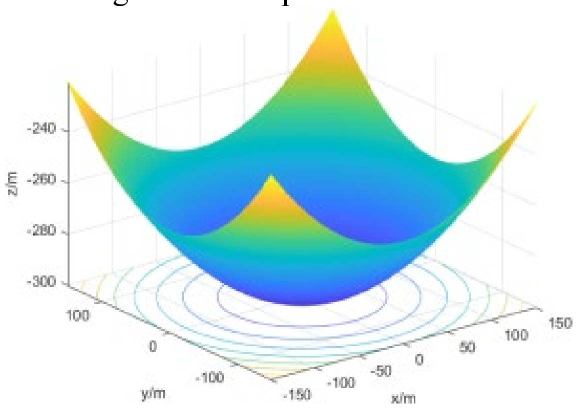

Figure 3. Ideal paraboloid top view

As can be seen in Figure 6, the fit of the ideal paraboloid to the reference sphere is high, and the scale limitation of the actuator retraction is difficult to be represented at the spatial scale of the illuminated area. Therefore, this paper makes a plot of the offset of the ideal paraboloid relative to the spherical surface as shown in Figure 4.

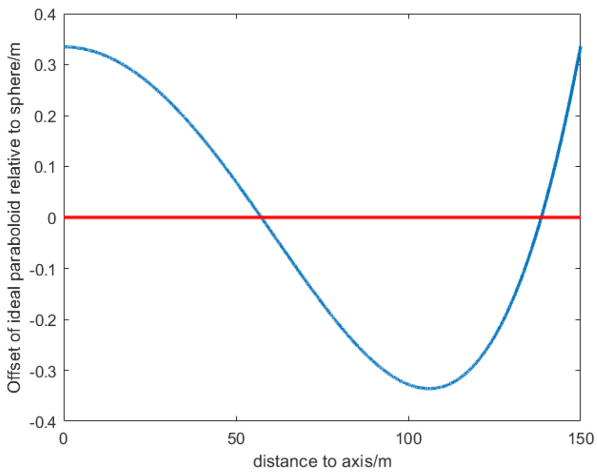

Figure 4. Plot of ideal paraboloid offset versus position with respect to the sphere

Analysis of results:

The optimum value for the maximum actuator expansion and contraction is $0.3360m$, which is less than the threshold value of $0.6m$ and satisfies the limits of the actuator expansion and contraction range. At the vertex, the paraboloid moves radially down by $0.3348m$; at the paraboloid boundary, the paraboloid moves radially down by $0.3360m$ The magnitude of the displacement of the ideal paraboloid with respect to the reference sphere tends to decrease and then increase with distance to the vertex.

2.2 Solution of the working parabolic optimization model

For the established working paraboloid optimization model, this paper uses the average distance corresponding to the main cable nodes as the guiding index for regulating the expansion and contraction of the decision variable actuator, and uses an iterative method to optimize the solution, and outputs the solution when the RMS stabilizes Results[8-10].

The algorithm flow chart for the solution is shown in Figure 5.

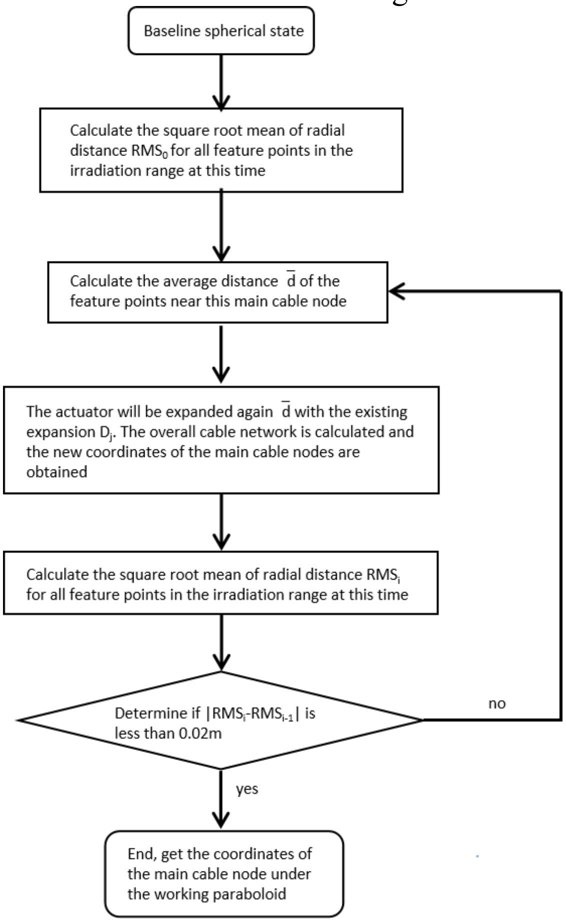

Figure 5. Algorithm flow diagram

The result obtained from the above solution is still the result in the new coordinate system, for which the coordinate transformation needs to be performed again to obtain the solution of the original problem.

$$\begin{bmatrix} x \\ y \\ z \end{bmatrix} = [AB] \begin{bmatrix} x' \\ y' \\ z' \end{bmatrix} \tag{22}$$

In the above equation, the left-hand side shows the coordinates of the solution to the original problem being solved, and the right-hand side shows the coordinates of the solution under the new coordinate system obtained so far.

Results:

The adjusted main cable node numbers and their coordinates (in part) obtained from the solution are given in Table 5.

Table 3. Table of main rope node numbers and coordinates Node number

Node number	the coordinates of X/m	the coordinates of Y/m	the coordinates of Z/m
$A0$	2.32913×10^{-5}	-7.89×10^{-6}	-300.40461
$B1$	6.108977121	8.40862326	-300.27803
$C1$	9.885927466	-3.2120491	-300.31831
$D1$	-2.72808×10^{-5}	-10.390895	-300.21714

$B2$	12.2122723	16.8093417	−299.77634
……	……	……	……
$B265$	184.522232	66.7869583	−227.84818
$B266$	188.3977978	54.9474672	−227.79445
$B267$	191.883948	43.1750335	−227.39879
$B268$	195.0358679	31.3137147	−226.66508
$B269$	197.8374122	19.441736	−225.59394

Table 4 gives the (partial) expansions for each actuator obtained by solving.

Table 4. Table of results for actuator expansion and contraction

Node number	actuator expansion and contraction/m
$A0$	−0.004521139
$B1$	−0.057903337
$C1$	−0.098154327
$D1$	0.00299455
$E1$	0.088489973
……	……
$B265$	−0.546997999
$B266$	−0.477570661
$B267$	−0.442519002
$B268$	−0.444925804
$B269$	−0.478140542

In order to visualize the results, a histogram of the actuator expansion and contraction is shown below.

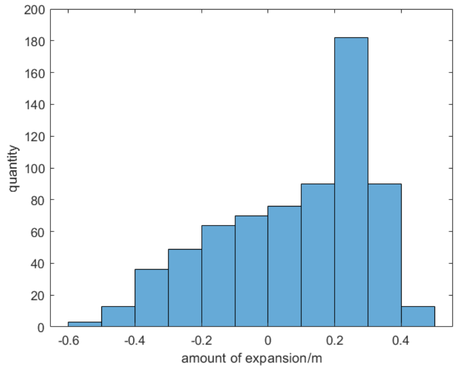

Figure 6. Histogram of actuator expansion and contraction

The graph shows that most of the nodes have a stretch between -0.4 and +0.4, which satisfies the constraint of 0.6 for the actuators given in the question and leaves enough margin. The largest number of nodes is between 0.2 and 0.3, while the rest of the segments are more evenly distributed.

3. Evaluation and extension of the model

3.1 Advantages of the model

In this question, the choice of using feature points in the calculation of the working paraboloid provides more detail to describe the closeness of the triangular reflective panel to the ideal paraboloid and enables a better description of the degree of fit. When optimizing the expansion of the actuators corresponding to the main cable nodes, we choose to use the average distance to determine the size of the next expansion, and gradually reduce the root mean square RMS by repeated iterations, which can sufficiently reduce the root mean square.

Analysis of experimental results

Due to the computational complexity of the algorithm, the number of iterations in problem 2 was small and the expected optimization was not fully achieved. When calculating the average distance in problem 2, the selection of the characteristic points does not take into account the fact that the dimensions of the six adjacent triangular plates are different, which may lead to a decrease in the solution effect when the dimensions of the triangular plates differ greatly.

4. Conclusions

In this paper, the method of selecting feature points is used to fit discrete triangular plates to a continuous surface, and the feature point method can be further extended to other problems. The movement of the main cable nodes in the tangential direction can be further considered for a more accurate solution.

References

[1] Cheng Qiyun, Sun Caixin, Zhang Xiaoxing, et al. Short-Term load forecasting model and method for power system based on complementation of neural network and fuzzy logic [J]. Transactions of China Electrotechnical Society, 2004, 19(10): 53-58.

[2] Nan Rendong. 500m spherical reflector radio telescope FAST[J]. Chinese Science G Series: Physics, Mechanics, Astronomy, 2005(05):3-20.

[3] Fangfang. Research on power load forecasting based on Improved BP neural network [D]. Harbin Institute of Technology, 2011.

[4] Amjady N. Short-term hourly load forecasting using time series modeling with peak load estimation capability [J]. IEEE Transactions on Power Systems, 2001, 16(4): 798-805.

[5] Ma Kunlong. Short term distributed load forecasting method based on big data [D]. Changsha: Hunan University, 2014.

[6] SHI Biao, LI Yu Xia, YU Xhua, YAN Wang. Short-term load forecasting based on modified particle swarm optimizer and fuzzy neural network model [J]. Systems Engineering-Theory and Practice, 2010, 30(1): 158-160.

[7] Ye Jingfei, Chen Yulin, Zhao Delin. Discussion on three-dimensional space reflection law based on Fermat's principle and its application [J]. Physics and Engineering, 2020,30(06):84-87+94.

[8] Qian Hongliang. Theoretical and experimental research on supporting structure of FAST reflector [D]. Harbin Institute of Technology, 2007.

[9] Shen Shizhao, Fan Feng, Qian Hongliang. Research on the overall scheme of the FAST active reflector support structure [J]. Journal of Building Structures, 2010, 31(12): 1-8. DOI: 10.14006/j.jzjgxb.2010.12.001.

[10] Jiang Peng, Wang Qiming, Zhao Qing. Optimization analysis and design of cable-net structure for giant radio telescopes [J]. Engineering Mechanics, 2013, 30(02): 400-405.